Project Title

MECHANISM OF THERMAL RUNAWAY IN VRLA BATTERIES AND METHODS TO SUPPRESS IT – PHASE II

FINAL TECHNICAL REPORT

BY

PROF. DETCHKO PAVLOV (PRINCIPAL INVESTIGATOR)
FULL MEMBER OF THE BULGARIAN ACADEMY OF SCIENCES

(MARCH 2007)

UNITED STATES ARMY

EUROPEAN RESEARCH OFFICE OF THE U.S. ARMY

LONDON, ENGLAND

CONTRACT NUMBER: N62558-06-P-0070

CONTRACTOR: INSTITUTE OF ELECTROCHEMISTRY AND ENERGY SYSTEMS (IEES)
LEAD-ACID BATTERIES DEPARTMENT

Approved for Public Release; Distribution Unlimited

Report Documentation Page

Form Approved
OMB No. 0704-0188

Public reporting burden for the collection of information is estimated to average 1 hour per response, including the time for reviewing instructions, searching existing data sources, gathering and maintaining the data needed, and completing and reviewing the collection of information. Send comments regarding this burden estimate or any other aspect of this collection of information, including suggestions for reducing this burden, to Washington Headquarters Services, Directorate for Information Operations and Reports, 1215 Jefferson Davis Highway, Suite 1204, Arlington VA 22202-4302. Respondents should be aware that notwithstanding any other provision of law, no person shall be subject to a penalty for failing to comply with a collection of information if it does not display a currently valid OMB control number.

1. REPORT DATE	2. REPORT TYPE	3. DATES COVERED
MAR 2007	**N/A**	**-**

4. TITLE AND SUBTITLE	5a. CONTRACT NUMBER
MECHANISM OF THERMAL RUNAWAY IN VRLA BATTERIES AND METHODS TO SUPPRESS IT PHASE II	5b. GRANT NUMBER
	5c. PROGRAM ELEMENT NUMBER

6. AUTHOR(S)	5d. PROJECT NUMBER
	5e. TASK NUMBER
	5f. WORK UNIT NUMBER

7. PERFORMING ORGANIZATION NAME(S) AND ADDRESS(ES)	8. PERFORMING ORGANIZATION REPORT NUMBER
UNITED STATES ARMY EUROPEAN RESEARCH OFFICE OF THE U.S. ARMY LONDON, ENGLAND	

9. SPONSORING/MONITORING AGENCY NAME(S) AND ADDRESS(ES)	10. SPONSOR/MONITOR'S ACRONYM(S)
	11. SPONSOR/MONITOR'S REPORT NUMBER(S)

12. DISTRIBUTION/AVAILABILITY STATEMENT
Approved for public release, distribution unlimited

13. SUPPLEMENTARY NOTES
The original document contains color images.

14. ABSTRACT

15. SUBJECT TERMS

16. SECURITY CLASSIFICATION OF:			17. LIMITATION OF ABSTRACT	18. NUMBER OF PAGES	19a. NAME OF RESPONSIBLE PERSON
a. REPORT **unclassified**	b. ABSTRACT **unclassified**	c. THIS PAGE **unclassified**	**SAR**	**23**	

Standard Form 298 (Rev. 8-98)
Prescribed by ANSI Std Z39-18

TABLE OF CONTENTS

Page

ABSTRACT

The aim of this project is to elucidate the mechanism of thermal runaway in VRLA batteries and especially the eventual role of the AGM separator. The oxygen evolution (OER) and oxygen recombination reactions (ORR) proceed in the cells, and the only work done by the input power is to transfer water from anode to cathode through these reactions, the remaining energy being dissipated as heat. The heat generators in the cell are the electrochemical reactions through their activation overpotentials, the exothermic chemical reactions and the exothermicity of ORR plus Joule Ohmic heating in electrolyte and solid phases. We have shown that, within the range of currents used (up to 1C), the major contribution comes from electrochemical reactions. The cell temperature is at most in a first order dependence of recombinant current. The OER at constant applied voltage and fixed ambient temperature is accelerated by the rise of internal cell temperature and overpotential, as the negative plate is depolarized by ORR due to enhanced separator permeability for oxygen flow by electrolyte displacement and/or drying and negative plate local desaturation. If the negative plate potential is stabilized at $Pb/PbSO_4$ potential and cannot be shifted by any current applied, the cell behaviour is controlled solely by OER reaction. Thus, a lower applied voltage is enough to produce a current sufficient to generate conditions for thermal runaway.

The range of overall active block saturations for stable behaviour is somewhere between 92% (where efficient recombination is possible) and 83-80% (where thermal runaway occurs immediately).

Modification of AGM separators (i.e. MAGM) could improve recombination and water retention at high saturations >92%, while for low saturations the newly developed modification MAGM II shows additionally a very promising effect of suppressing thermal runaway phenomena even at saturations below 80%. In MAGM II cells the thermal runaway excursion to boiling is moved beyond the positive grid corrosion failure point.

The results obtained in this study suggest strongly that by modification of separator properties it is possible to achieve better thermal control, in concert with other cell design improvements, plus the usual external measures as power input management and passive/active cooling.

INTRODUCTION

In order to be able to control a given phenomenon it is of utmost importance to disclose the mechanism(s) of its action and of the processes involved. In the case of valve-regulated lead-acid batteries (VRLAB) a very important factor is the saturation of battery cells with electrolyte. The degree of electrolyte saturation is responsible for the proportion between the gas channels along which oxygen flows and liquid (hydrophilic) channels along which the flows of H^+ and SO_4^{2-} ions, and water move between the two types of plates in the cell. The processes of oxygen reduction proceed at the negative (lead) plates and these are exothermic processes. In the first phase of the TRA project (contract number: N62558-03-M-0805), it was established that reduction of oxygen and its recombination to water might proceed through a combination of electrochemical and chemical reactions [1-5]. These reactions take place at the negative plates. As these are exothermic reactions, the temperature in the cell rises and may reach values beyond the temperature range of normal battery operation, which will shorten battery cycle life. It was established further that the reactions at the two types of plates (electrodes) might get into a self-accelerating interrelation. This interrelation results in rapid increase of cell current (i.e. of the rate of the electrochemical reactions) and of cell temperature to values that may lead to battery failure or impair substantially the performance of the battery. This phenomenon is called "thermal runaway" (TRA).

In the previous reporting period (2nd Interim Report) we have established that TRA occurs when the electrolyte saturation in the cell falls down below 80% [6,7]. The major volume of electrolyte is absorbed in the AGM separator. Hence, the latter's properties, pore distribution by radius and thickness, will exert a strong influence on the occurrence of the TRA phenomenon during VRLAB operation.

In the last reporting period we investigated the influence of separator type and thickness on VRLAB operation. AGM separator supplied by Hollingsworth & Vose (USA) and modified AGM separator (MAGM) were used for these investigations. MAGM was produced employing a technology developed by the team of the Lead-Acid Batteries Department at the Institute of Electrochemistry and Energy Systems (IEES) of the Bulgarian Academy of Sciences (US Patent: 6,509,118 B1 [8]).

Cells were assembled with AGM and MAGM separators of two different thicknesses. It has been established that separator type affects the occurrence of TRA. In an attempt

to facilitate manifestation of this effect, the polymer emulsion originally used for separator modification (MAGM) was substituted with a new one with different formula (MAGM II). Initial tests and investigations of the thermal phenomena in cells with MAGM II separators were performed and the results obtained are most encouraging.

EXPERIMENTAL SET-UP

All experiments were performed with 4 Ah test cells comprising two positive and three negative plates. Two types of separators were used: absorptive glass mat (AGM) and modified absorptive glass mat (MAGM) separators. The thickness of the separators was also varied. Four test cells were assembled: two cells with AGM separator - one with 3 mm thickness of the separator and one with 4.8 mm, respectively; and two cells with MAGM separator – again one with 3 mm and one with 4.8 mm separator thickness. The thicker separator comprised two sheets of 2.4 mm AGM or MAGM separator attached to one another. For the sake of simplicity we will refer to the four cells as AGM3, AGM2x2.4, MAGM3 and MAGM2x2.4. The separator sheets were placed both between the positive and negative plates, and between the box walls and the outermost negative plates in order to prevent free oxygen access directly to the bare negative plate surface and subsequent fast oxygen reduction, as well as dry-out of the outer negative plates. All experiments were carried out at room temperature.

The equipment used was:
- Bitrode SCN 10-5 test modules used to maintain constant current or constant voltage in the model cells;
- Ag/Ag_2SO_4 reference electrode designed in this laboratory;
- 16-channel computerized data acquisition system;
- Thermocouples mounted on the cell walls;
- Computerized gassing rate monitoring (GRM) system (own design).

Cell current (I), voltage (U), positive and negative plate potentials (φ^+ and φ^-) temperature (T) and released gas (in terms of number of gas bubbles per unit time, *dN/dt)*, were monitored during the experiments.

EXPERIMENTAL RESULTS AND DISCUSSION

1. Cycling test at $U = 2.60$ V

During the previous reporting period (2nd Interim Report) we performed cycling test experiments at $U = 2.65$ V. The higher applied voltage was chosen in order to provoke faster dry-out of the cell and subsequent faster occurrence of TRA phenomena so as to determine the critical electrolyte saturation level. It has been established that TRA phenomena start when the electrolyte saturation of the cell falls down below 80%. Under such extreme conditions all processes of formation of gas channels in the separator, of electrolyte redistribution and cell dry-out are very fast. Hence, the influence of separator type and thickness, which determine the transport of ion species and management of water between the electrodes, cannot be studied.

In the present cycling test the applied voltage is reduced to $U = 2.60$ V. In this way the influence of separator on TRA can be investigated.

First the four test cells AGM3, AGM2x2.4, MAGM3 and MAGM2x2.4 were set to cycling comprising two steps: 6 hours of polarization at constant voltage $U = 2.60$ V, followed by a 6-hour rest period to allow cooling of the cell to room temperature. Before cycling, the cells were charged at constant current $I = 0.2$ A for 10 hours and then left on open circuit for 2 hours.

The initial electrolyte saturation of all cells was 96%. This initial saturation was achieved by an established procedure: first the cells were filled with electrolyte to 100% saturation and then, through sucking of electrolyte, the saturation was reduced to the desired level.

1.1. Characteristic profiles of cell current, temperature and potential for a single polarization pulse

The cycling test for AGM3 and MAGM3 cells comprised 120 cycles and that for AGM2x2.4 and MAGM2x2.4 cells, 80 cycles. Because of the long duration of the experiment the evolution of cell parameters with time cannot be presented in single graphs. Hence, the obtained results are summarized in terms of characteristic values for the individual cell parameters as a function of number of cycles. The profiles of cell

current, temperature and plate potentials during a single polarization pulse are presented in Fig. 1.
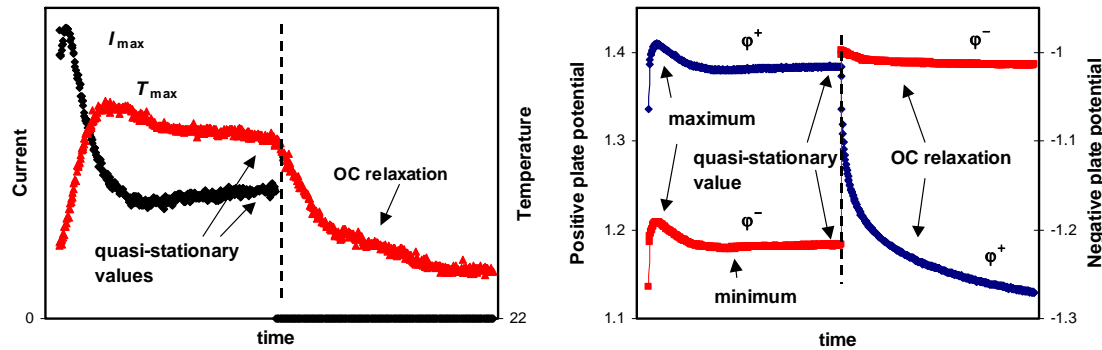
Fig. 1. Characteristic profiles of I, T, φ^+ and φ^- during single polarization step followed by open circuit relaxation.

Figure 1a shows that on switching polarization on the cell current passes through a maximum first and then decreases reaching a quasi-stationary value at the end of the polarization step. Peak sharpness and time for establishing steady-state regime vary during the experiment.

The cell temperature also passes through a maximum, which is broader and flatter than that for I, and at the end of polarization the temperature goes to quasi-stationary value (see Fig.1a). Both current and temperature maximums can be attributed to some structural changes in the cell related to the formation of gas channels in the separator facilitating oxygen transport between the plates. After this period the closed oxygen cycle (COC) is operative. In this experiment temperature variations are small because the generated cell current is very low (see Fig. 3 in Section 1.2.). During the open circuit (OC) period, T relaxes to room temperature. From the relaxation curve the thermal capacity and convective heat transfer coefficient can be evaluated.

Figure 1b presents the characteristic profiles of positive and negative plate potential pulses. Both potentials pass through maximums, then through minimums and reach stationary values thereafter. In the beginning of polarization the first two reactions that proceed at the negative plate are reduction of residual $PbSO_4$ to Pb and evolution of H_2. The maximum in φ^- is a result of the former reaction. After certain time, $PbSO_4$ is reduced and O_2 reaches the negative plate, hence φ^- does not increase further. The potential minimum and the quasi-stationary value of φ^- are determined by the competition between the oxygen and hydrogen reactions. Initially, the hydrogen

reaction is predominant. With time of polarization the amount of oxygen that reaches the negative plate increases and O_2 reduction becomes determining for the potential value: φ^- goes to less negative values.

As temperature variations in this experiment are very small (up to 5-10°C, see next chapter) the positive plate potential profile is determined entirely by the negative one. Both potentials are interrelated through the applied constant voltage.

For interpretation of the experimental data from the cycling test we will discuss the evolution of the quasi-stationary values of the cell parameters with number of cycles in the next chapter.

1.2. Influence of separator type and thickness

All cells lost water during the experiments. The changes in electrolyte saturation *vs.* number of cycles are presented in Fig. 2.
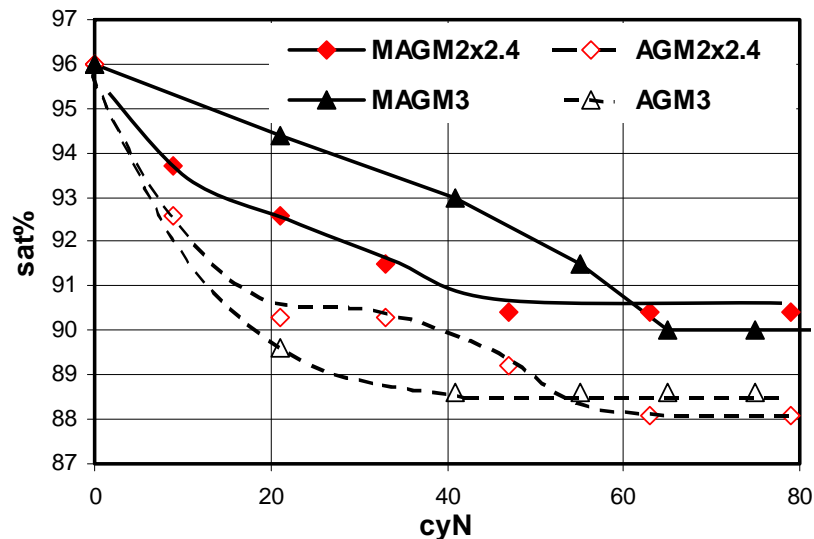

Fig. 2. Changes of cell saturation during cycling test experiment

The initial saturation of the cells was 96%. Judging by the saturation *vs.* cycle number curves two stages in cell behaviour can be distinguished: non-stationary one and stationary one. During the stationary stage the saturation of the cells with electrolyte does not depend on separator thickness. The stationary saturation level for both AGM cells is reached after 54 cycles and for both MAGM cells after 63 cycles. The corresponding stationary saturation levels are 88.3% for AGM cells and 90.2% for MAGM cells, respectively. The cells with MAGM separator lost less water compared to

cells with AGM separator. This was due to the facilitated transport of oxygen through the MAGM separator due to the latter's hydrophobic channels. Hence, cells with this type of separator start to operate in regime of recombination at higher saturations. This was also demonstrated during the non-stationary stage of water loss, in which MAGM cells lost less water and retained higher saturation levels than AGM cells. MAGM3 cell had the highest recombination rate and it maintained the highest saturation level during the non-stationary period.

Figure 3 presents the changes in stationary values of cell current, I_{st} vs. number of cycles for the four test cells. At the beginning of the cycling test I_{st} for AGM3 cell is 0.08 A (Fig. 3a). Between 15th and 30th cycles the cell undergoes a transition period and I_{st} increases to 0.2 A. This transition period is in correlation with the cell dry-out. Electrolyte saturation decreases below 90% and more gas channels for oxygen transportation between the electrodes are formed. Figure 4a shows that the greater amount of O_2 that reaches the negative plate causes the negative plate potential φ^- to shift towards less negative values: φ^- changes from -1.29 V to -1.21 V. Due to the interrelation between φ^- and φ^+ through the applied voltage the positive plate potential increases from 1.31 V to 1.39 V (Fig. 4b). The latter leads to enhanced oxygen evolution and subsequent cell current increase. After this transition period the electrolyte saturation of the cell remains constant but I_{st} creeps up smoothly to the end of the experiment reaching 0.3 A.

Figure 3a indicates a slightly different behaviour of MAGM3 cell. In general, of the cells with 3 mm thick separators the one with MAGM separator sustains higher current (0.6 A). This is due to the fact that MAGM separator allows faster formation of gas channels, even at higher electrolyte saturations, due to its special processing (modification). Hence, MAGM3 cell operates in regime of higher oxygen recombination at any saturation level compared to AGM3 cell. This finding is clearly demonstrated by the potential curves in Figs. 4a and 4b. Throughout the cycling test, the negative electrode of MAGM3 cell is more depolarized than that of AGM3 cell. In the case of MAGM3 cell, $\varphi^- = -1.21$ V at the beginning of the experiment and it goes to -1.14 V with cell dry-out. This difference between AGM3 and MAGM3 cells is more pronounced at higher saturations. The smooth decrease of I_{st} of MAGM3 cell up to the 50th cycle correlates with the decrease of ambient temperature (Fig. 5).
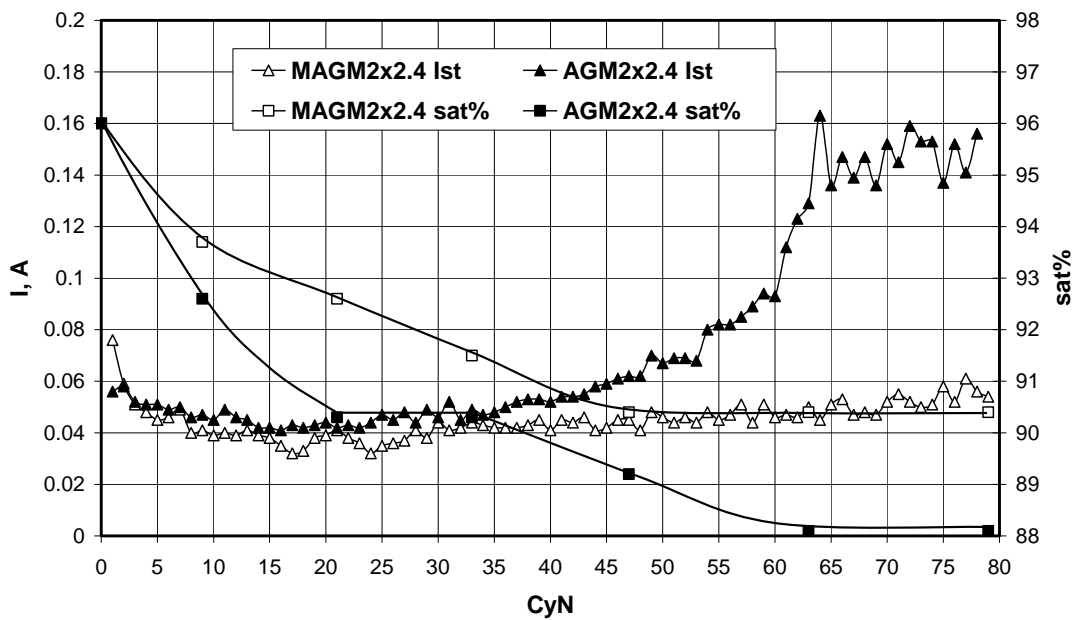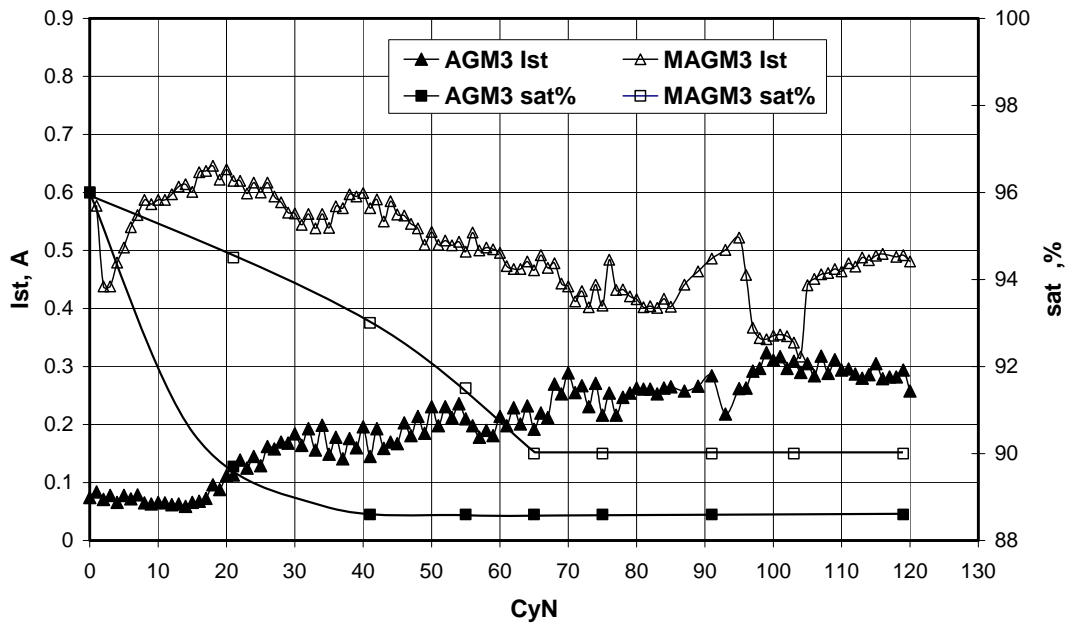
Fig. 3. Changes of cell current and saturation with number of cycles:
a) AGM3 and MAGM3 cells; b) AGM2x2.4 and MAGM2x2.4 cells

10
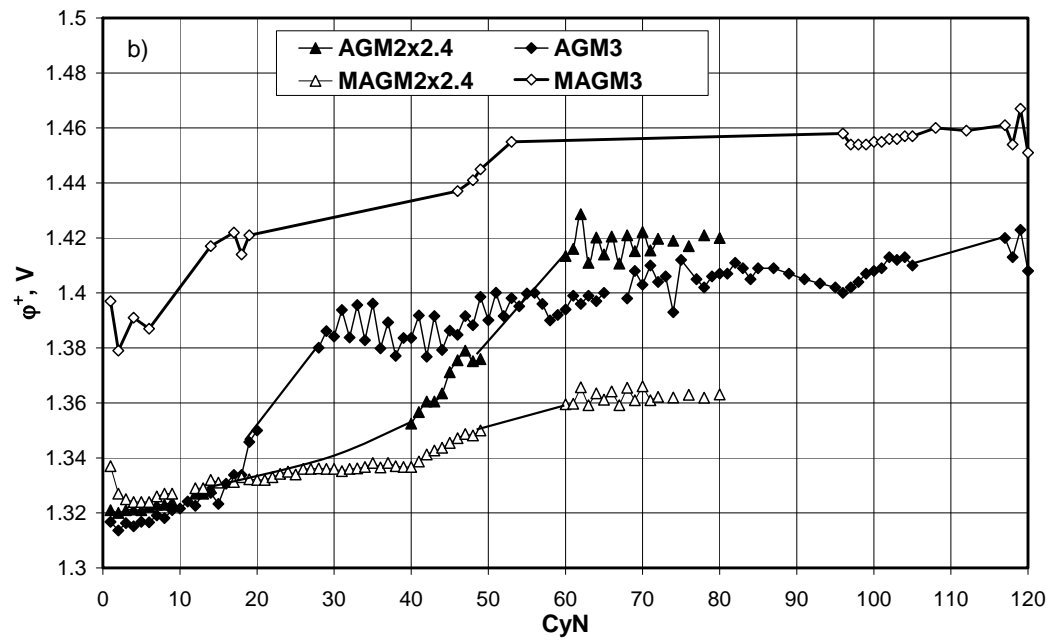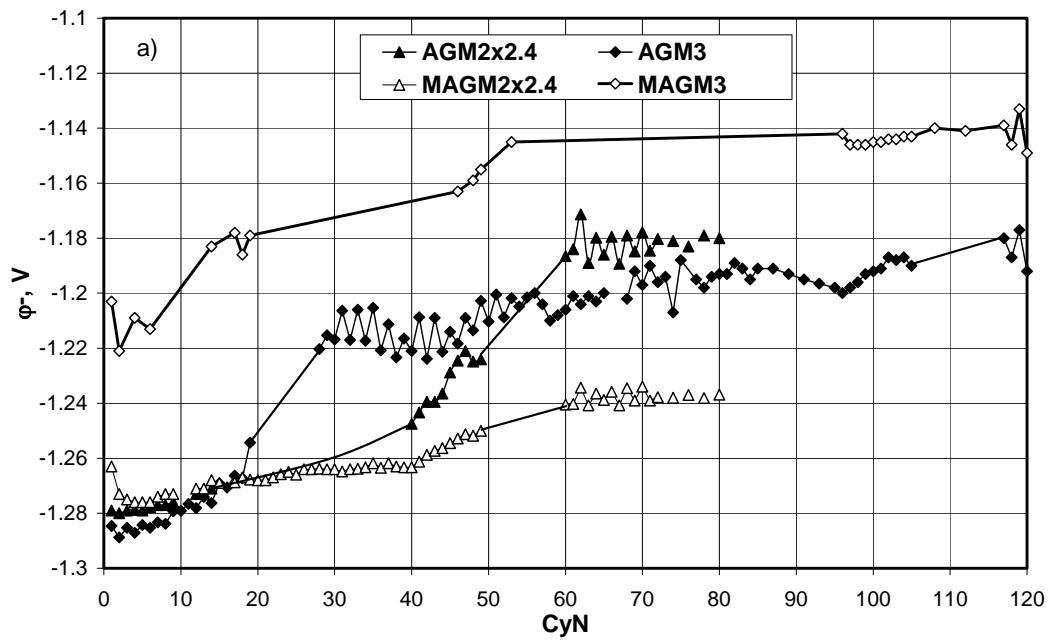
Fig. 4. Changes of negative and positive plate potentials with number of cycles

On grounds of the data in Figs. 3a and 4 the following conclusions can be drawn for the influence of separator type on the performance of AGM3 and MAGM3 cells:

During COC operation MAGM3 cell has more depolarized negative plate than AGM3 cell. It corresponds to higher polarization of the positive plate and higher rate of oxygen evolution in MAGM3 cell. Hence, MAGM3 cell operates at higher current compared to AGM3 cell (Fig. 3a). As COC is more efficient in cells with MAGM separator the water loss of MAGM3 cell will be lower than that of AGM3 cell and the cell with MAGM separator will sustain higher saturation level.

Let us now look at the behavior of the cells with thicker separator. During the first 40 cycles the current of both AGM2x2.4 and MAGM2x2.4 cells is around 0.05 A (Fig. 3b). This current is an order of magnitude lower than that of MAGM3 cell. After 40th cycle, I of AGM2x2.4 cell starts to increase and reaches a stationary value of 0.15 A during 65th cycle. It is interesting to note that I of MAGM2x2.4 cell stays very low and almost constant for all 80 cycles of the test (Fig. 3b). If we compare this behavior with the changes in electrolyte saturation it can be seen that for AGM2x2.4 cell when the saturation level falls below 90% more channels for transport of O_2 between the electrodes are open, which accelerates the oxygen reduction rate and I increases. Figure 3b evidences that the changes of saturation between 96% and 90.5% for MAGM2x2.4 cell do not affect the cell current. During the first 20 cycles the negative plate potentials of both AGM2x2.4 and MAGM2x2.4 cells are very close (around -1.27; -1.28 V). Then φ^- of AGM2x2.4 cell starts to decrease and reaches -1.18 V at 60th cycle. This change in negative plate potential is related to the increase of cell current from 0.06 A to 0.15 A. The negative plate of MAGM2x2.4 cell also depolarized between cycles 40 and 60, but the change of φ^- is only 40 mV in this case, which has but insignificant influence on cell current (Fig. 4a).

The above results indicate that AGM2x2.4 cell is very sensitive to changes in electrolyte saturation, especially for saturations lower than 90%. Below that saturation level a substantial depolarization of the negative plate occurs, which leads to an increase of positive plate potential and to three-fold increase in cell current.

The changes in saturation between 96% and 90% do not affect the electrochemical behavior of the two cells with MAGM separator (MAGM3 and MAGM2x2.4). This

difference between the cells with MAGM and AGM separators is due to the specific treatment of MAGM separator that changes the surface properties of its fibers.

Figure 5 presents the changes in temperature difference between cell and ambient temperatures (T-T_a) during the experiment. The ambient temperature is also given in the Figure. The temperature differences for the cells with thick separators are not presented because they are less than 2^oC due to the very low current values. The heat generation for AGM2x2.4 and MAGM2x2.4 cells is negligible. It is seen from the graphs that (T-T_a) for cells with 3mm thick separator follows the respective cell current behavior and is a direct consequence of I.
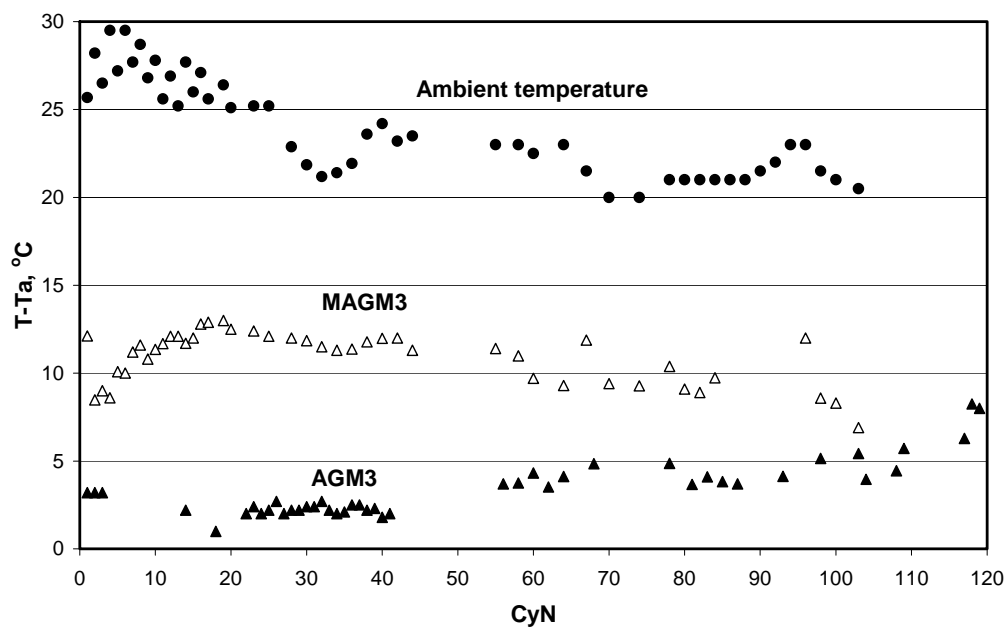
Fig. 5. Changes of $T - T_a$ and ambient temperature with number of cycles.

2. Step-wise constant voltage polarization

Figure 3 shows that at the end of the cycling test at U = 2.60 V the currents of all four cells reach stationary values. Hence, every cell has a characteristic current for the reached stationary saturation values and applied voltage 2.60 V. Table 1 summarizes the final stationary saturation levels and cell currents for the four cells under test. The question is what will be the behavior of the cells at the same saturations but at lower applied voltages?

Table 1. Saturation levels and cell currents at the end of the cycling test at $U = 2.60$ V

	AGM3	MAGM3	AGM2x2.4	MAGM2x2.4
Saturation	88.6%	90%	88.1%	90.4%
I_{st}, A	0.3	0.45	0.15	0.05

The following experiment was set up: first the cells were set to constant voltage polarization at $U = 2.60$ V for 16h; then the voltage was changed stepwise (by 0.05 V per step) to U = 2.35 V. The duration of each step was 8 h. The experiment was repeated twice for the sake of consistency. The variations of cell current, positive and negative plate potentials with time were monitored.

Figure 6 shows the changes in cell current with time for AGM3 and MAGM3 cells. When AGM3 cell is polarized at $U = 2.60$ V, its current I passes through an initial maximum, followed by a minimum at 0.15 A and starts to increase thereafter reaching 0.34 A after 16 h of polarization. At $U = 2.60$ V, the current of MAGM3 cell reaches its stationary value of 0.45 A. With decreasing the polarization voltage the current of both cells decreases. For both cells I cannot reach quasi-stationary value within the time of polarization and the experiment demonstrates very long current relaxation times, τ. The possible reasons for these long relaxation times are impeded transport of O_2 through the separator, diffusion through the thin liquid film adjacent to the electrode surface or adsorption relaxation time. The first two reasons are hardly possible. At the saturation levels of this experiment (Table 1), gas penetration channels for O_2 transport between the electrodes are easy to form. The characteristic time for this process is around 1 to 3 hours depending on the saturation. The characteristic time for diffusion of O_2 molecules through 100 μm thick film is of the order of 10^{-5} s. Therefore, the only possible reason for relaxation time of the order of 20 h is barrier limited adsorption. The problem of long relaxation time needs further investigations.
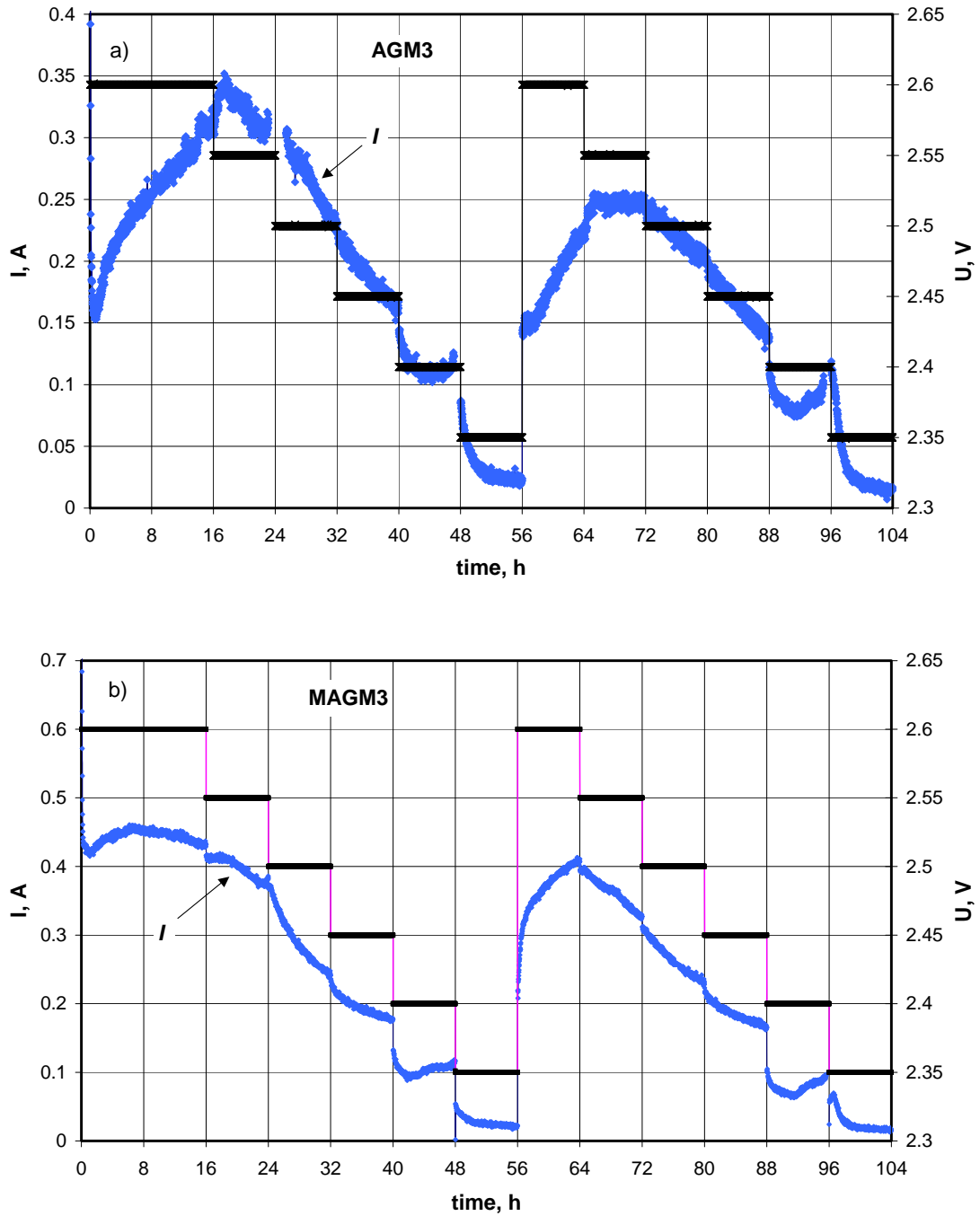
Fig. 6. Cell current during step-wise constant voltage polarization: a) AGM3 cell;
b) MAGM3 cell

Figure 7 shows the changes in positive and negative plate potentials for AGM3 and MAGM3 cells during the stepwise constant voltage polarization experiment.
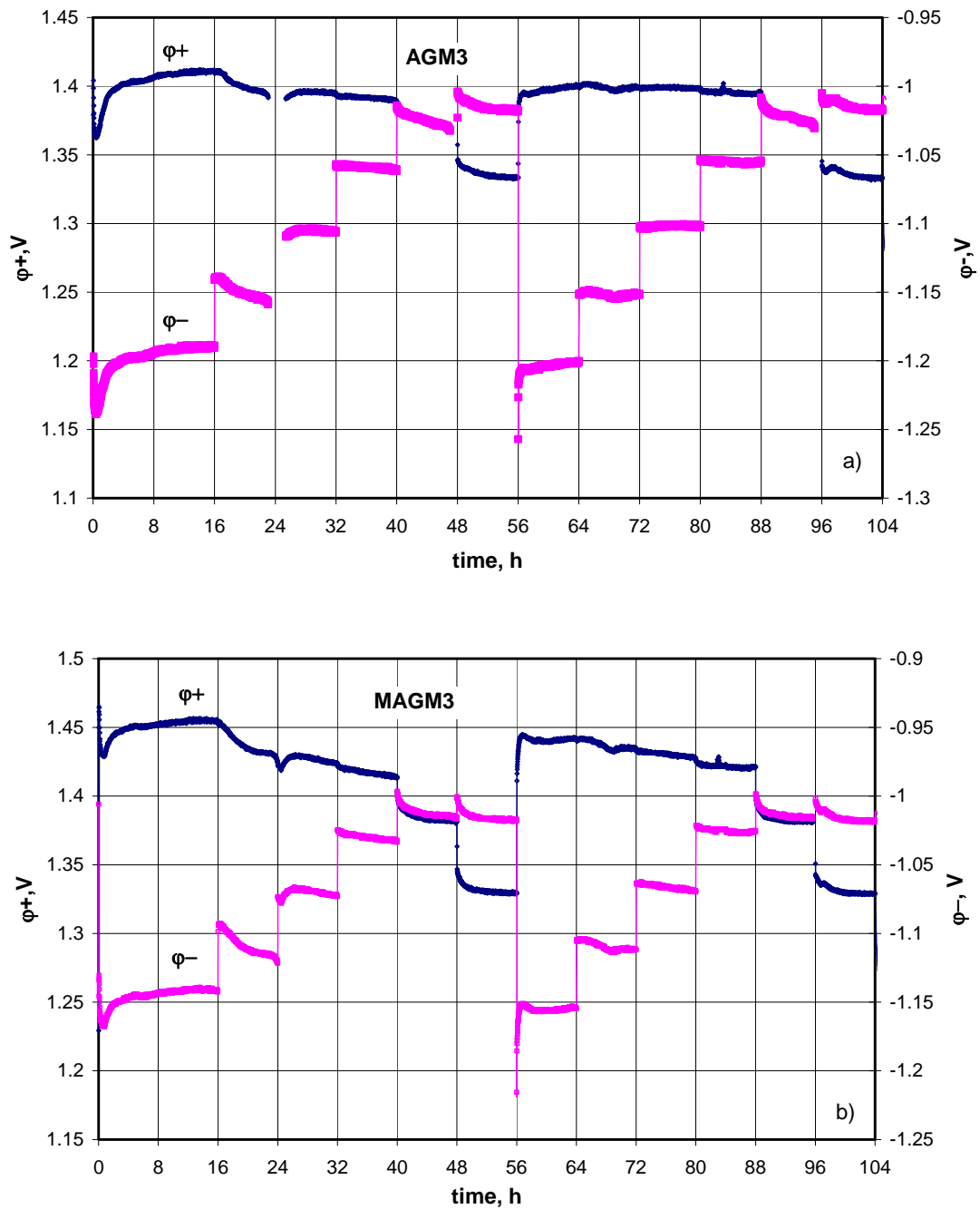
Fig. 7. Positive and negative plate potentials during step-wise constant voltage polarization: a) AGM3 cell; b) MAGM3 cell.

At $U = 2.60$ V, both electrodes are polarized in both cells ($\varphi^+ \approx 1.40$ V and $\varphi^- \approx -1.20$ V for AGM3 cell and $\varphi^+ \approx 1.45$ V and $\varphi^- \approx -1.15$ V for MAGM3 cell, respectively). During the period of current increase the positive electrodes polarize while the negative ones

depolarize. During the subsequent stepwise decrease of U down to 2.35 V, the behavior of φ^+ and φ^- of both AGM3 and MAGM3 cells is similar:

(a) AGM3 cell: at applied voltages from 2.60 V to 2.40 V, φ^+ decreases slightly from 1.42 V to 1.38 V. The changes of U affect only φ^-, i.e. the negative electrode depolarizes stepwise. The negative plate potential changes by 160 mV and reaches values of −1.030 V at $U = 2.40$ V. The stationary potential of the negative plate is within the range from −1.010 V to −1.03V. When this potential is reached, further changes in applied voltage ($U \leq 2.40$ V) affect positive plate potential, which changes step-wise by approximately 50 mV. Hence, $U = 2.40$ V appears to be a critical applied voltage. When $U > 2.40$ V, the positive electrode is the potential determining one with constant polarization and the changes in U affect only φ^-. On the contrary, for $U \leq 2.40$ V, the negative electrode is the potential determining one and only φ^+ changes with U.

(b) MAGM3 cell: $U = 2.40$ V is a critical applied voltage for this cell, too. The stationary potential of the negative plate is −1.020 V and is more pronounced. Hence, $U = 2.40$ V appears to be a critical transition voltage, which most probably plays an important role for the cell behaviour. Elucidation of this phenomena requires further experimental investigations.

Figures 8 and 9 present the experimental data for I, U, φ^+, and φ^- for cells with thick separators (AGM2x2.4 and MAGM2x2.4). On changing the polarization voltage the cells with 4.8 mm thick separator have completely different behavior from the cells with 3 mm thick separator. Like the cells with 3 mm separator, when polarized at 2.60 V the currents of AGM2x2.4 and MAGM2x2.4 cells have stationary values, I_{st}. However, in contrast to the cells with thinner separator, here there is a region of applied voltages for which I increases with decrease of polarization voltage for both AGM and MAGM cells. For AGM2x2.4 cell, the current passes through a maximum at $U = 2.50$ V and then decreases with further decrease of U. The data for MAGM2x2.4 cell presented in Fig. 8b show that I stays constant ($I = 0.06$ A) for applied voltages from 2.60 V to 2.50 V. With further decrease of U to 2.45 V, I starts to increase, passes through a maximum and then decreases with lower applied voltages. During the second run of the step-wise constant voltage polarization the current increase starts at higher polarization voltage $U = 2.50$ V.
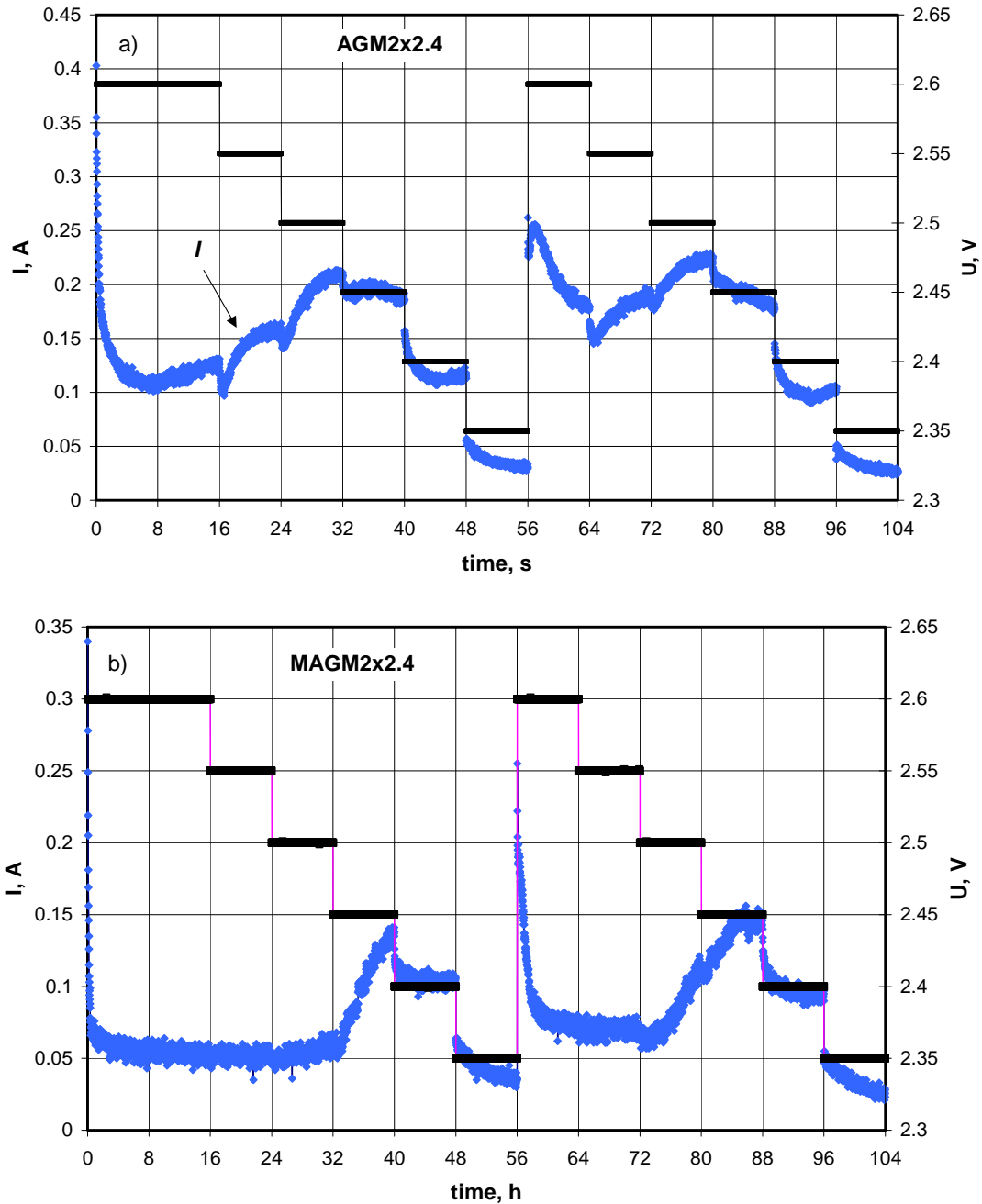
Fig. 8. Cell current during step-wise constant voltage polarization: a) AGM2x2.4 cell; b) MAGM2x2.4 cell.

Figure 9 presents the experimental data for φ^+ and φ^- vs. time for the step-wise constant voltage polarization experiment. It can be seen from the figure that at higher polarization voltages φ^+ stays constant or increases, which leads to strong depolarization of the negative potential. Similar to the cells with 3 mm thick separator, when AGM2x2.4 and MAGM2x2.4 cells are polarized at U = 2.40 V and 2.35 V, φ^- is

closer to the OC potential of Pb electrode and subsequent changes of U affect only φ^+. Hence, for cells with thick separators $U = 2.40$ V is a critical transition voltage at which the negative electrode becomes independent and the changes in applied voltage affect the polarization of the positive plate only. A comparison between the data in Figs. 7 and 9 evidences that the critical transition voltage $U = 2.40$ V does not depend on separator type and thickness.
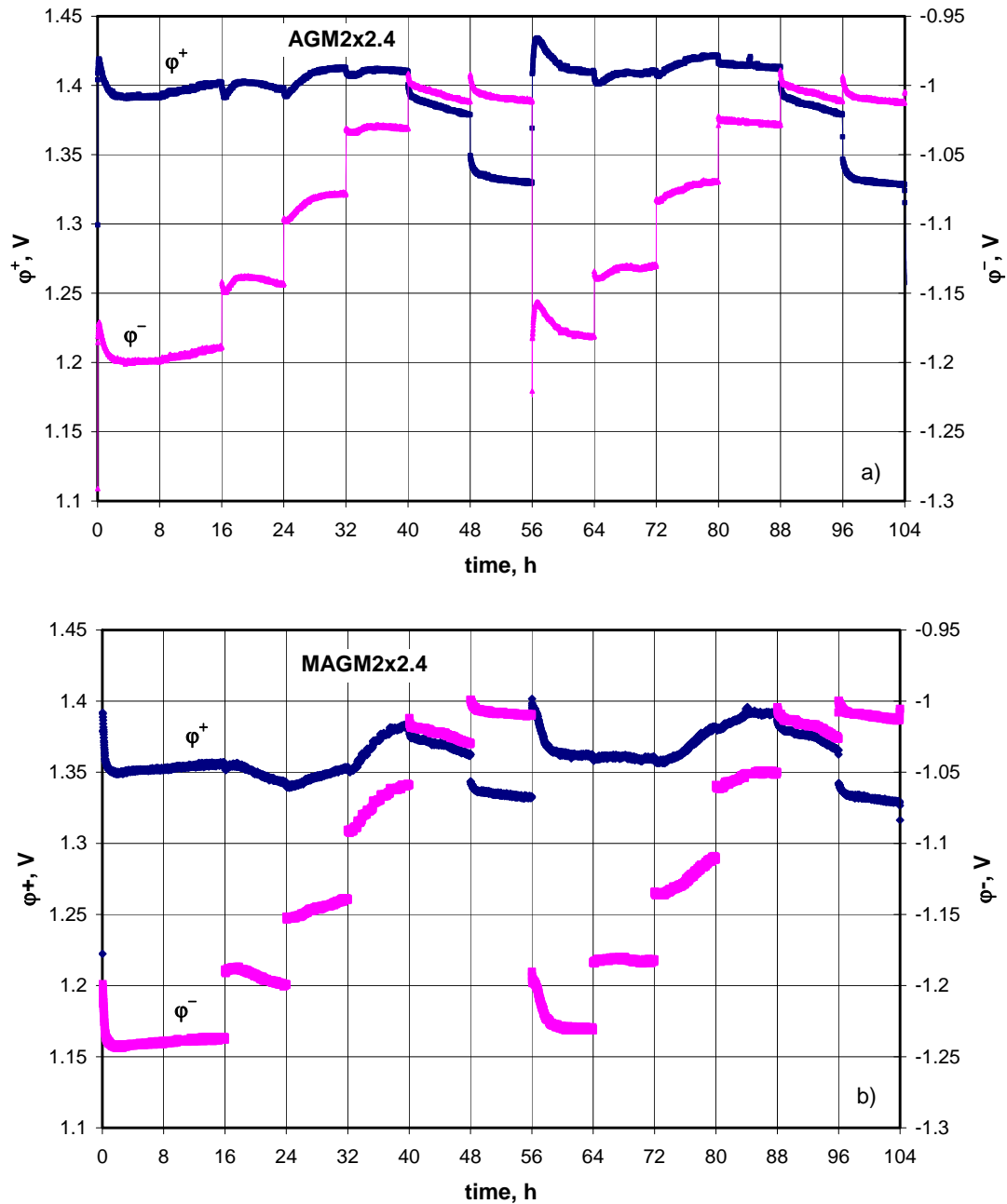
Fig. 9. Positive and negative plate potentials during step-wise constant voltage polarization: a) AGM2x2.4 cell; b) MAGM2x2.4 cell

It follows from the above discussion that evolution of the negative plate passes through two stages during oxygen cycle operation: a) stationary or depolarized stage, when $\varphi^- \approx$ -1.020 V, and b) polarized stage when $\varphi^- > |$-1.020 V$|$.

It can be seen from the data in Fig. 8 that, for given periods of time when polarization voltage decreases the cell current increases. In an attempt to explain this behavior we have plotted the quasi-stationary values of φ_{st}^+ and φ_{st}^- vs. I (Figs. 10 and 11). For the polarization steps at which I does not reach stationary value we have taken the I value at the end of polarization.
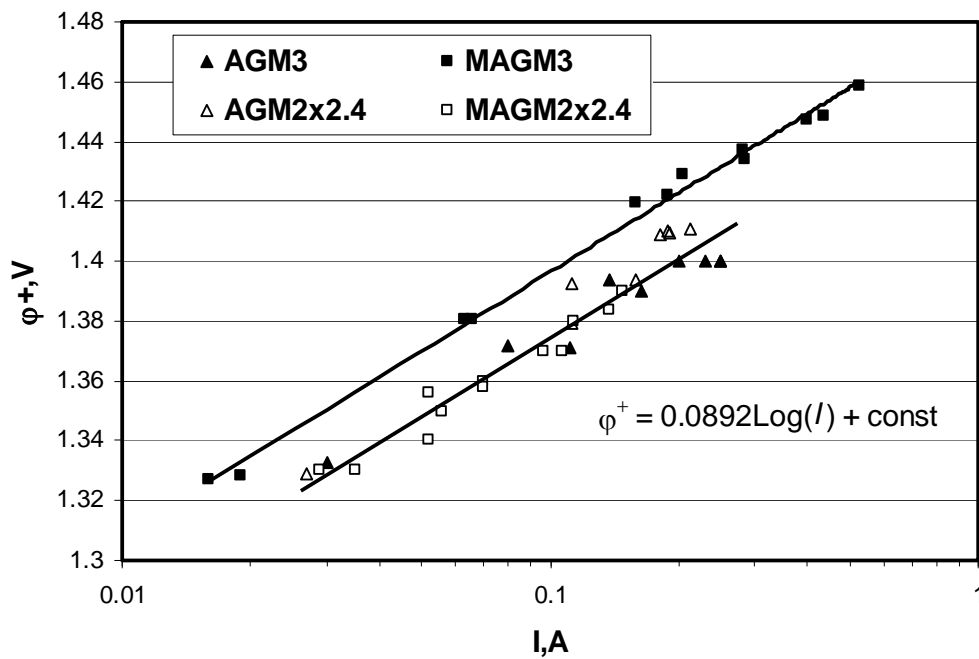
Fig. 10. Positive plate potential as a function of cell current during step-wise constant voltage polarization.

As expected, Fig. 10 shows that the positive plate potentials of all four cells obey the Tafel equation and do not depend on separator thickness or type:

$$\varphi^+ = 0.0892 \log(I) + \text{const} \qquad (1)$$

The slope is 89.2 mV per decade, which corresponds to the value for oxygen evolution reaction. At the positive plate only the electrochemical reaction of oxygen evolution proceeds. For a given polarization voltage the negative plate potential determines the

value of the positive plate potential, which settles the cell current following Tafel equation (1).

Figure 11 presents the obtained I vs. φ_{st}^{-} curves for the four cells under test and the two subsequent step-wise voltage series.
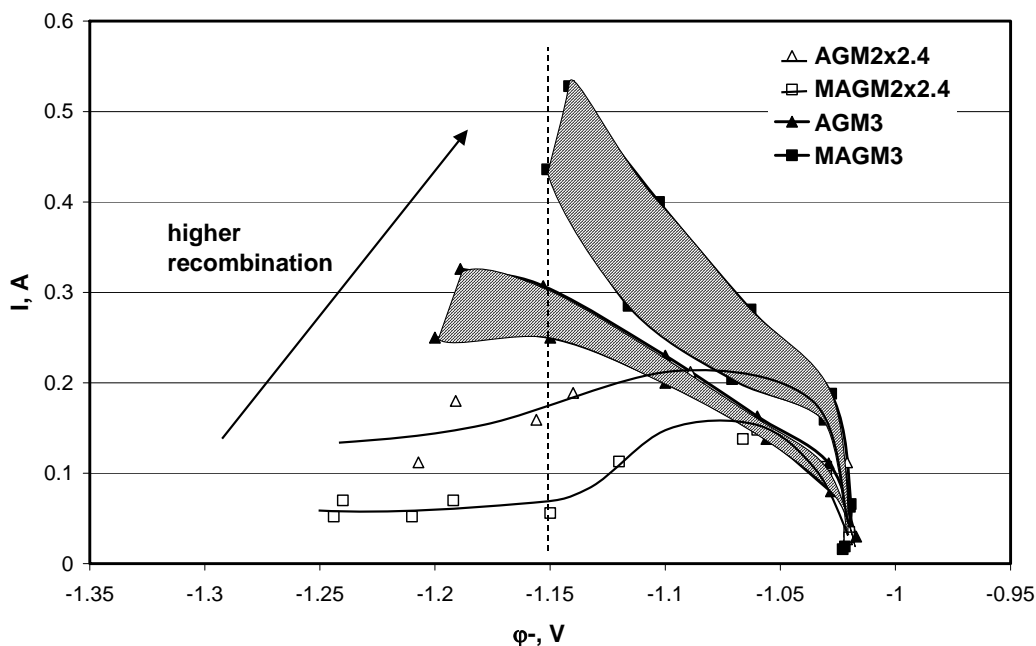
**Fig. 11.** Cell current vs. negative plate potential during step-wise constant voltage polarization.

The following conclusions can be drawn from the graphs:

a) For the cells with thicker separator the dependence of I on φ_{st}^{-} for both step-wise voltage series are very close, which means that within the 8 hours of polarization the processes at the negative plate reach stationary state. This is not the case with the thinner separator cells. There are two I vs. φ_{st}^{-} curves for the AGM3 cell. Up to -1.1 V, the two curves are very close, but at more negative φ_{st}^{-} values the difference becomes wider. For MAGM3 cell the two curves are considerably apart from each other at potentials lower than -1.030V, which may be a result of some structural changes in the negative plate that may cause different reactions to proceed during the first and second polarization series.

b) Separator thickness and type exert substantial influence on the rates of the reactions that proceed at the negative plates. For the cells with thinner separators the reactions proceed at higher rate in the cell with MAGM3

21

separator, while for the cells with thick separator the reactions are faster in the AGM2x2.4 cell. This finding should be taken into account when designing VRLAB. Thick separators have higher resistance towards O_2 transport between the two electrodes, hence the current of such cells is substantially lower than the current of cells with thin separators.

c) I vs. φ_{st}^- curves for cells with thick separators are stationary. With decreasing φ_{st}^- to -1.08 V the cell current increases, hence, its value is determined by the electrochemical reactions at the negative plate. For $\varphi_{st}^- <$ -1.08 V, I for both cells decreases and becomes almost constant at $\varphi_{st}^- <$ -1.150 V. This behavior is an indication of changes in the type of reactions that proceed, which can be caused by the products formed at the Pb active mass/solution interface. If we draw a straight line at $I = 0.1$ A for MAGM2x2.4 cell and at $I = 0.2$ A for AGM2x2.4 cell it can be seen that the same current can be achieved at two different potentials. This means that different reactions proceed therein. Hence, there are two potentials at which the electrochemical reactions proceed at the same rate at the negative plate. In other words, the processes that proceed at the negative plate have two quasi-stationary states at two different potentials. These finding suggest that there are two competitive reactions. Such reactions can be H_2 evolution and O_2 reduction. Figure 11 evidences also that I is constant at potentials lower than -1.15 V. This can be due to diffusion limited processes or to chemical reactions that appear to be dominant. In order to disclose the mechanism of this bi-stability of the system further investigations are needed.

d) For cells with thin separators the volt-ampere curves have different slopes that depend not only on separator type but also on polarization series. This means that the reactions taking place at the negative plate depend on separator type and thickness. A scheme of the possible reactions that proceed at the negative plate (presented also in our previous reports) is given in Fig. 12. It is not possible to judge from the potential curves alone which reaction will proceed at the electrode within a given potential range. Additional experimental methods need to be applied in order to determine the type(s) of reaction(s) operative in a given potential interval.

$$⑨ \; 2H \rightarrow H_2$$

$$⑤ \; 2H^+ + 2e^- \rightarrow 2H$$

$$⑧ \; H_2O_2 + 2H \rightarrow 2H_2O + (-383.2 \; kJ/mol)$$

$$⑥ \; O_2 + 2H^+ + 2e^- \rightarrow H_2O_2$$

$$⑦ \; H_2O_2 + 2H^+ + 2e^- \rightarrow 2H_2O$$

$$⑩ \; H_2O_2 \rightarrow H_2O + \tfrac{1}{2}O_2 + (-97.38 \; kJ/mol)$$

$$⑪ \; Pb + H_2O_2 \rightarrow Pb(OH)_2 + (-326.2 \; kJ/mol)$$

$$⑬ \; Pb(OH)_2 + 2e^- + 2H^+ \rightarrow Pb + 2H_2O$$

$$⑭ \; Pb(OH)_2 \rightarrow 2H_2O + PbO + (+159.0 \; kJ/mol)$$

$$⑮ \; Pb(OH)_2 + H_2SO_4 \rightarrow PbSO_4 + 2H_2O + (-89.6 \; kJ/mol)$$

$$⑯ \; PbSO_4 + 2e^- + 2H^+ \rightarrow Pb + H_2SO_4$$

$$⑰ \; 4Pb(OH)_2 + H_2SO_4 \rightarrow 3PbO.PbSO_4.H_2O + 4H_2O + Q$$

$$⑫ \; 2Pb + O_2 + 2H_2O \rightarrow 2Pb(OH)_2 + (-457.6 \; kJ/mol)$$
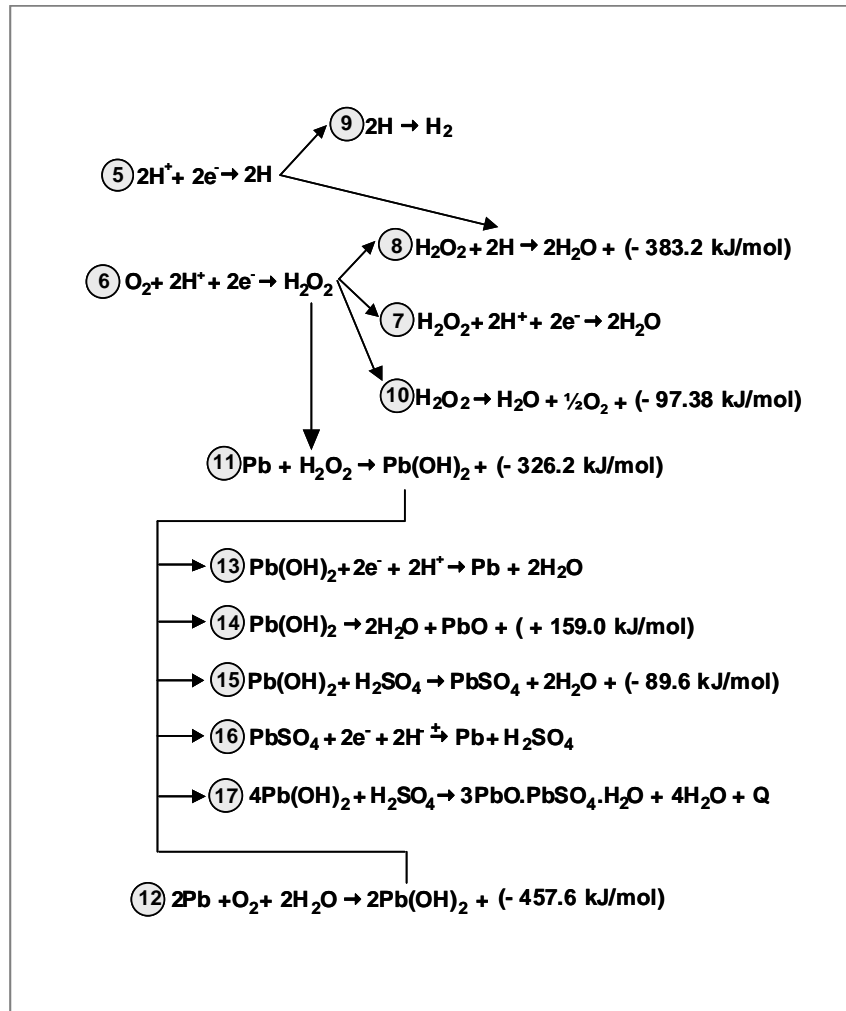
Fig. 12. Scheme of the chemical and electrochemical reactions involved in the reduction of oxygen at the negative plates [4].

3. Transition between polarized and depolarized state of negative plate at constant current polarization

In an attempt to study in detail the bi-stable behavior of cells with 4.8 mm thick separators and to try to elucidate the processes involved we performed the following experiment with MAGM2x2.4 cell. The changes in φ^-, φ^+, U and gassing rate were monitored and the obtained results are presented in Fig. 13.